AD NUMBER

AD479898

LIMITATION CHANGES

TO:

Approved for public release; distribution is unlimited.

FROM:

**Distribution authorized to U.S. Gov't. agencies and their contractors;
Administrative/Operational Use; 20 DEC 1965.
Other requests shall be referred to Office of Naval Research (ONR), One Liberty Center, 875 North Randolph Street, Arlington, VA 22203-1995.**

AUTHORITY

ONR ltr dtd 12 Dec 1975

December 20, 1965

TRANSDUCERS USING FORCED TRANSITIONS BETWEEN FERROELECTRIC AND ANTIFERROELECTRIC STATES

by

Don A. Berlincourt

Clevite Corporation
Electronic Research Division
Cleveland, Ohio

Engineering Memorandum 65-23

Presented at IEEE, 1965 Ultrasonics Symposium,
Boston, Massachusetts, December 3, 1965

Work reported herein supported by Office of
Naval Research Contract Nonr 3958(00) and
Sandia Corporation (AEC) contract 53-2206.

DISCLAIMER NOTICE

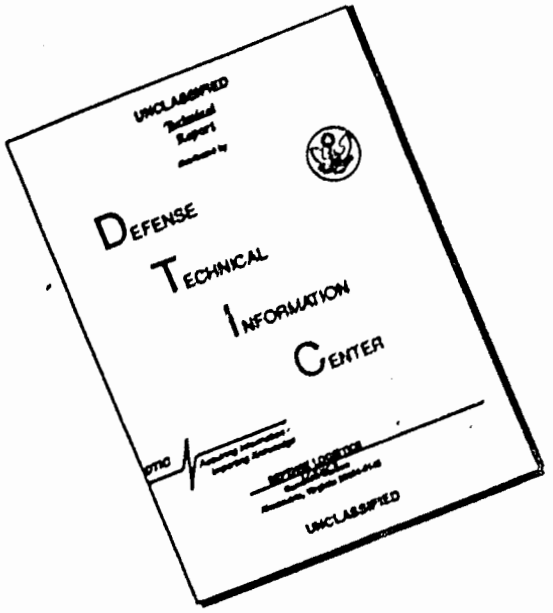

THIS DOCUMENT IS BEST QUALITY AVAILABLE. THE COPY FURNISHED TO DTIC CONTAINED A SIGNIFICANT NUMBER OF PAGES WHICH DO NOT REPRODUCE LEGIBLY.

TRANSDUCERS USING FORCED TRANSITIONS BETWEEN FERROELECTRIC AND ANTIFERROELECTRIC STATES*

By

D. Berlincourt
Clevite Corporation, Electronic Research Division
Cleveland, Ohio

ABSTRACT

The use of resonant piezoelectric composite structures for acoustic radiation into fluid media is well established. At low frequencies, desirable for long distance acoustic transmission, resonant structures are extremely large and expensive. Frequency lowering can be accomplished by a variety of means involving use of bending structures or mass-loading, but the resulting transducers are vulnerable to pressure effects due to deep submersion. A possible alternative to present transducer structures is the use of the electric field-forced transition from antiferroelectric to ferroelectric. A number of $Pb(Zr, Sn, Ti)O_3$ compositions have been developed which experience these transitions at relatively low electric field (~ 7-15 kV/cm) and typically generate volume strains near 0.1%. There is therefore not necessarily a requirement for acoustic shielding, and since the developed strain is independent of frequency, resonant structures are not needed. Construction is therefore simplified and the size and weight of low frequency transducers may be reduced. Operating characteristics of the antiferroelectric transducer are discussed in detail, but no large low frequency transducer arrays have yet been built.

INTRODUCTION

The transition antiferroelectric-ferroelectric can occur spontaneously with temperature change, increase in electric field, or change in stress configuration. The technically important ferroelectric ceramic materials with

---

*Presented at 1965 IEEE Ultrasonics Symposium, Boston, Massachusetts, December 3, 1965.

the exception of $PbNb_2O_6$ are all of the perovskite structure type and are therefore only slightly distorted from cubic. Some of these materials have both ferroelectric and antiferroelectric distorted structures, and in these cases transitions to ferroelectric from either cubic (paraelectric) or antiferroelectric involve an increase in specific volume. The specific volume of the cubic state is intermediate between that of the ferroelectric and antiferroelectric states. In the ferroelectric state the unit cell is elongated parallel to the polar axis; in the antiferroelectric state one of the axes perpendicular to the antiparallel displacements is shorter than in the cubic (reference) phase.

It has been demonstrated that hydrostatic and one-dimensional compression favor the antiferroelectric state, and transitions at pressures as low as a few thousand psi have been obtained with some compositions.[1, 2] The pressure-forced transition may be used for conversion of mechanical to electric energy. In similar fashion the electric field-forced antiferroelectric-ferroelectric transition may be used for conversion of electrical to mechanical energy by virtue of the geometric change of the primitive unit cell. Since the transition occurs also with temperature change, thermoelectric and thermomechanical energy conversion are also possible. With respect to the heat of transition these processes are directly coupled, but the thermal energy required to provide the necessary temperature rise limits power conversion to the 1% efficiency range.

The electric field-forced transition was demonstrated first in $PbZrO_3$ by Shirane, et al.[3] in a narrow temperature range near the Curie point. Sawaguchi showed that substitution of about 3 atom% Ti^{4+} for Zr^{4+} in $PbZrO_3$ introduces a ferroelectric state (rhombohedral) in a narrow temperature range below the Curie point.[4] The electric field-forced antiferroelectric-ferroelectric

---

[1] D. Berlincourt, H. Jaffe, H. H. A. Krueger, and B. Jaffe, "Release of Electric Energy in $PbNb(Zr, Ti, Sn)O_3$ by Temperature and by Pressure-Enforced Phase Transitions," Appl. Phys. Letters 3, pp. 90-92, Sept. (1963).

[2] D. Berlincourt, H. H. A. Krueger, and B. Jaffe, "Stability of Phases in Modified Lead Zirconate with Variation in Pressure, Electric Field, Temperature, and Composition," J. Phys. Chem. Solids, Vol 25, pp. 659-674 (1964).

[3] G. Shirane, E. Sawaguchi, and Y. Takagi, Phys. Rev. 84, 476-481 (1951).

[4] E. Sawaguchi, J. Phys. Soc. Japan 8, 615-629 (1953).

transition in $Pb(Zr, Ti)O_3$ compositions is obtained only over a narrow temperature range because the free energy of the ferroelectric state is slightly higher than that of the antiferroelectric state only over a narrow temperature range. B. Jaffe found that this difference in free energy is minimized over a much wider temperature range by substantial substitution of Sn^{4+} for $(Zr, Ti)^{4+}$, [5] and that further reductions are accomplished by substitution of La^{3+} and Sr^{2+} for Pb^{2+}. [6]

GENERAL PRINCIPLES OF THE ANTIFERROELECTRIC TRANSDUCER

The equations which define the action of the antiferroelectric transducer are derived readily from the thermodynamic potential generally called the Gibbs free energy. The antiferroelectric-ferroelectric transition is a first order transition, and there are therefore discontinuities in the partial derivatives of the Gibbs free energy with respect to temperature, stress, or electric field. These partial derivatives are respectively entropy, mechanical strain, and dielectric displacement. The following relationships are obtained by setting the Gibbs free energy equal for states A and F. They hold for first order transitions, with derivatives taken along the phase boundaries.

$$\left(\frac{\partial E}{\partial p}\right)_\theta = \frac{\Delta V/V}{\Delta D} \quad , \tag{1}$$

$$\left(\frac{\partial \theta}{\theta E}\right)_p = -\frac{\theta \Delta D}{\Delta Q} \quad , \quad \text{and} \tag{2}$$

$$\left(\frac{\partial p}{\partial \theta}\right)_E = \frac{\Delta Q}{\theta \Delta V/V} \quad , \quad \text{where} \tag{3}$$

E = electric field (V/m),
D = dielectric displacement (C/m^2),
θ = temperature (°K),
p = hydrostatic pressure (N/m^2), and
ΔQ = thermal energy (J/m^3, heat of transition).

---

[5] B. Jaffe, Proc. IRE 49, 1264 (1961).

[6] B. Jaffe, unpublished.

These equations hold strictly only for equilibrium conditions, but actually there is always hysteresis. It has nevertheless been shown that the equations hold well especially for transitions occurring with <u>increasing</u> temperature, pressure, or electric field.[2]

Equation (1) describes the action of the ferroelectric transducer for electrical to mechanical energy conversion or vice versa. Equations (2) and (3) describe the action in thermoelectric and thermomechanical conversion, and will not be discussed further here. Equation (1) can be generalized to include stress systems other than hydrostatic pressure as follows:

$$\left(\frac{\partial E_3}{\partial T_3}\right)_{\theta, T_1, T_2} = \frac{\Delta S_3}{\Delta D_3} \quad , \quad \text{and} \tag{4}$$

$$\left(\frac{\partial E_3}{\partial T_1}\right)_{\theta, T_2, T_3} = \frac{\Delta S_1}{\Delta D_3} \quad , \quad \text{where} \tag{5}$$

S_3, S_1 = strain parallel and perpendicular to applied electric field and

T_3, T_1 = stress parallel and perpendicular to applied electric field (N/m^2)

For increments in stress and electric field with the appropriate boundary conditions, Equations (1), (4), and (5) become

$$\Delta E \, \Delta D = (\Delta V/V)\Delta P \, , \tag{6}$$

$$\Delta E \, \Delta D = \Delta S_3 \, \Delta T_3, \quad \text{and} \tag{7}$$

$$\Delta E \, \Delta D = \Delta S_1 \, \Delta T_1 \, . \tag{8}$$

These equations state that a compressive stress raises the transition electric field to ferroelectric and that an electric field will likewise raise the transition stress to antiferroelectric, and that the energies involved are equal. This is equivalent to stating that these energies are perfectly coupled, k = 100%.

Figure 1 illustrates the ideal equilibrium (no hysteresis)field-forced ferroelectric transition at ambient (for practical purposes zero) pressure. The transition to ferroelectric at the electric field E_t is marked by an increase in polarization ΔP and specific volume $\Delta V/V$. With decrease in electric field the transition back to the stable antiferroelectric phase takes

place here also at E_t. Under nonequilibrium conditions there is significant hysteresis and the transition fields for the transitions to ferroelectric (E_f) and to antiferroelectric (E_a) are related $E_a < E_t < E_f$.

Figure 2 shows schematically the actual operation of the antiferroelectric transducer for electromechanical energy conversion. D-E and ΔV-p plots are sketched for three conditions of mechanical load: a) zero pressure load, b) linear mechanical load with energy dissipated in the load, and c) ideal nonlinear mechanical load. With a) there is no energy conversion and a volume change ΔV occurs at E_f, a change $-\Delta V$ at E_a with electric field decrease. The dielectrically dissipated energy per unit volume W_D is given approximately by

$$W_D = (E_f - E_a)P_S \quad , \tag{9}$$

where

P_S = spontaneous polarization of the ferroelectric state, C/m^2,

E = electric field, V/m, and

W_D = dissipated energy density, J/m^3.

In b) the mechanical energy/unit volume delivered is $W_M \sim 1/2\ (\Delta V/V)\Delta p$. The additional electrical energy dissipated is $1/2\ \Delta E\ \Delta D = 1/2\ (\Delta V/V)\Delta p$ (see Eq. (6)). With the ideal nonlinear load the mechanical energy delivered is $\Delta p(\Delta V/V) = \Delta E\ \Delta D$.

With the linear mechanical load the ratio of energy delivered to energy dissipated in the antiferroelectric element is

$$W_{Delivered}/W_{dissipated} = \frac{1/2\ \Delta E}{E_f - E_a} \quad . \tag{10}$$

Under these ideal conditions the efficiency is

$$e = \frac{1}{1 + 2\,\dfrac{E_f - E_a}{\Delta E}} \quad . \tag{11}$$

This shows that the key to efficient operation is low hysteresis ($E_f \sim E_a$) and heavy loading (ΔE large). This will be discussed further with respect to data on actual ceramic compositions, but it should be noted that the antiferroelectric transducer cannot be highly efficient. Its strength lies rather

in simplicity of design and freedom from the requirement of mechanical resonance. It should perhaps be noted that the treatment has to this point been general, not limited to a fluid load. The antiferroelectric transducer is better matched, of course, to solid loads. One could, for instance, use an antiferroelectric transducer (low duty cycle) for generation of high amplitude acoustic waves at any frequency below its switching speed (at least 5 Mc with the best materials). It can thus be used as an extremely broadband (dc to a few Mc) delay line transducer or as a generator of elastic stress for elasto optic modulation, but in both cases with a severely restricted duty cycle.

Figure 3 shows schematically the operating range of a "slanted" loop antiferroelectric transducer. A dc bias field about equal to the average of E_f and E_a is maintained and an ac electric field is applied to generate the volume strain. The resulting ac polarization and ac strain are shown schematically. Due to nonlinearity and hysteresis the dynamic polarization and strain are distorted. The distortion in the polarization results in internal heating (Equation 9), while that in strain results only in distortion of the acoustic signal. The latter results in some degradation of output power at the driving frequency, but does not otherwise affect operation.

EXPERIMENTAL DATA

There are two antiferroelectric states in modified and unmodified $PbZrO_3$, one with orthorhombic symmetry with only very slight distortion from tetragonal, the other with tetragonal symmetry. In each case there is very high cell multiplicity, with over 100 perovskite unit cells in one tetragonal multiple cell. The forced transition to ferroelectric occurs generally only from the tetragonal antiferroelectric state. $PbZrO_3$ is orthorhombic antiferroelectric at room temperature. The temperature-composition phase diagram of Fig. 4 shows that this state remains stable to the Curie point. Substitution of substantial amounts of Ti^{4+} for Zr^{4+} [4] (Fig. 4), Ba^{2+} for Pb^{2+}, [7] or Nb^{5+} for Zr^{4+} [8] brings about a ferroelectric (rhombohedral)

---

[7] G. Shirane and S. Hoshino, Acta. Cryst. 7, 203 (1954).

[8] N. N. Krainik, Zh. Tekh. Fiz. 28, 525 (1958)

phase. Three ferroelectric phases are shown in Fig. 4. The tetragonal ferroelectric phase F_T is isostructural with $PbTiO_3$. There is a first order transition between the two rhombohedral phases, with discontinuities in lattice constants and polarization, but it has not yet been possible to detect any superstructure in either state or a difference in symmetry.[9, 2]

Substitution of Sn^{4+} for $(Zr, Ti)^{4+}$ and/or La^{3+} for Pb^{2+} in $Pb(Zr, Ti)O_3$ extends the tetragonal antiferroelectric state at the expense of the rhombohedral ferroelectric state. These effects are demonstrated in triaxial phase diagrams in Figs. 5 and 6. In addition, Fig. 5 shows the establishment of a metastable $F_{R(LT)}$-A_T phase boundary by poling. With compositions within the metastable region the forced transition from antiferroelectric to ferroelectric occurs with electric field increase, but the ferroelectric state remains as a metastable phase with removal of the electric field. An example of this type of behavior is shown in Fig. 7.

Only compositions which have the tetragonal antiferroelectric state stable over a useful temperature range may be considered for application as antiferroelectric transducers. For the transition to occur at a reasonable electric field the free energy difference should be low. This in effect means that desirable compositions are those which are close to the $F_{R(LT)}$-A_T phase boundary in phase diagrams such as Figs. 5 and 6, and on the A_T side.

The differences in primitive cell volumes for the $F_{R(HT)}$, A_O, A_T, and cubic (paralectric) phases are illustrated by the thermal expansion curves in Figs. 8 and 9. These curves and other related data show that the primitive unit cell size is in the following order:

1. A_O
2. A_T
3. P
4. $F_{R(LT)}$
5. $F_{R(HT)}$*

Volume increasing ↓

---

(9) H. Barnett, J. Appl. Phys. 33, 1606 (1962).

*The high temperature ferroelectric rhombohedral phase does not occur in Figs. 8 and 9, and it does not in fact exist in compositions exhibiting the forced transition over a wide temperature range.

The specific volume difference A_O-$F_{R(HT)}$ is as high as 0. 96%, but this transition cannot be electric field-forced. The transition which can be field-forced in specific compositions over a wide temperature range is that between A_T and $F_{R(LT)}$. The specific volume difference ranges from 0. 5% to less than 0. 1% depending on composition. It should be noted that thermal expansion in the ferroelectric range is markedly anisotropic with poled specimens. This is much more pronounced in $F_{R(HT)}$ than $F_{R(LT)}$.

Figure 10 shows dimensional changes through a pressure-forced ferroelectric-antiferroelectric transition for the composition whose thermal expansion curve is shown in Fig. 8. The upper curves show S_1 and S_3 for a poled specimen and the curve at lower right shows $\Delta V/V = 2S_1 + S_3$. Remanent values of S_1 and S_3 are due to domain orientation, and remanence in $\Delta V/V$ for the poled specimen is the result of a slight volume increase, probably due to microcracks, which occurred during poling. The pressure at which the transition $F_{R(LT)}$-A_T occurs is more sharply defined in the poled specimen, and it occurs at a pressure about 8, 000 psi higher. This should be expected since the electric energy stored in poling ($\int$ edD) raises the energy difference between the ferroelectric and antiferroelectric states, causing a similar increase in mechanical energy ($\int$p dV/V) required to force the transition. The electric energy stored is about equal to $E_c\ P_R$ = 0. 19 J/cm^3. The additional mechanical energy is about equal to $\Delta p\ \Delta V/V$ = 0. 23 J/cm^3.

Figure 11 shows an electric field-pressure phase diagram for the composition whose thermal expansion curve is shown in Fig. 8 and whose dimensional changes through the pressure-forced transition $F_{R(LT)}$-A_T are shown in Fig. 10. These data were obtained by measurement of transiition pressure, determined from permitttivity-pressure curves,* at different bias electric field levels. The slope of p_a (pressure for transition to antiferroelectric with increasing pressure) vs. bias field curve is 960 psi/kv/cm. Using this and P_R = 27 μC/cm^2, Equation (1) gives $\Delta V/V$ = 0. 41%, in nearly exact agreement with the value obtained in Fig. 10 and the value extrapolated

*Permittivity is markedly higher in the ferroelectric state.

to room temperature in Fig. 8. The upper curve in Fig. 11 is asymmetric about zero electric field because of the original polarity of the poled specimen.

There are in general terms two different types of electric field-forced antiferroelectric-ferroelectric A_T-$F_{R(LT)}$ transitions. Neither, of course, has the ideal characteristics sketched in Fig. 1. Typical charge density-electric field hysteresis loops for the two types are shown in Fig. 12. All antiferroelectric Pb(Zr, Sn, Ti)O_3 compositions with Curie points above about 100°C appear to have either relatively "square" or "slanted" hysteresis loops. In comparison with the "square" loop materials, those with "slanted" loops have lower transition electric fields (E_f), lower relative volume differences between the ferroelectric and antiferroelectric states, wider temperature ranges over which the transition can be forced by electric field, and much less hysteresis. Furthermore, the forced transition is faster with the "slanted" loop materials, taking place in less than one microsecond. All factors other than the magnitude of the volume difference thus favor the "slanted" loop materials for acoustic power generation.

Typical strain-field curves for transitions of these two types are shown in Figs. 13 and 14. The strains S_1 perpendicular to and S_3 parallel to the electric field are shown as well as $S_V = S_3 + 2S_1$. The strain S_1 was measured by means of a strain gage cemented to an electroded surface. The volume strain S_V was determined from volume displacement of the specimen when placed inside a small oil-filled fused quartz chamber with a calibrated capillary. The strain S_3 was calculated ($S_3 = S_V - 2S_1$).

Several of the advantages of the "slanted" loop composition for acoustic power generation are immediately evident in Fig. 12 and demonstrated by comparison of Figs. 13 and 14, as well as the disadvantage of considerably lower transition strain. The first one-half cycle is unique, and is shown here only for completeness. There is a small remanence in S_3 and S_1, with that in the former opposite in sign and almost exactly twice the magnitude of the latter. The remanence is due to domain orientation in the forced ferroelectric state, and because of the mechanical nature of this orientation its effects remain in the stable antiferroelectric state. It is necessary to heat the specimen above the Curie point to remove the remanent strains, and only after doing so can the first one-half cycle be repeated. For use in transducers this is not important, and in any case there is no such effect with the volume strain.

It is noteworthy and of considerable practical importance that with the "slanted" loop material the strain S_1 is more than an order of magnitude less than S_3. On repetitive cycling S_1 even contributes to the volume strain, but only slightly. In contrast piezoelectric ceramic transducers presently employed in radiating transducers generate maximum strain at or near mechanical resonance, and require acoustic shielding to prevent strain cancellation due to cross-contraction. This in addition to the necessity for frequency lowering and impedance matching leads to high static stress and consequent large changes in the parameters of the piezoelectric ceramic.[10-16]

Figure 15 shows volume strain as a function of polarization for the "slanted" loop composition. This curve essentially combines the data of the hysteresis loop in Fig. 12 and the volume strain-electric field curve in Fig. 13. The curve in Fig. 15 is virtually linear within the transition region (to $P \sim 18\ \mu C/cm^2$). With $P \gtrsim 18\ \mu C/cm^2$, there are piezoelectric effects in addition to further transition effects. Near P_S there are no additional transition effects, and the piezoelectric effect reaches its saturation value ($g_h \sim 17 \times 10^{-3}\ m^2/C$).

Figure 16 shows corresponding data for the pressure-forced transition ferroelectric-antiferroelectric. The curve at the left is reproduced from Fig. 10. The curve in the center shows loss of polarization of the ferroelectric state through the transition, with the indicated initial slope equal to the measured values of d_h. The loss of polarization is shown as a function of $\Delta V/V$ on the right. Just as in Fig. 15, the $\Delta V/V$-P relationship is linear through the transition region.

---

(10) D. Berlincourt and H. H. A. Krueger, J. Appl. Phys. 30, 1804 (1950).

(11) B. A. Rotenberg, Soviet Phys.–Solid State 1, 1627 (1960).

(12) H. H. A. Krueger and D. Berlincourt, J. Acoust. Soc. Am. 33, 1339 (1961).

(13) S. V. Bogdanov, B. M. Vul, and R. Ya. Razbash, Soviet Phys.–Cryst. 6, 58 (1961).

(14) R. F. Brown, Can. J. Phys. 39, 741 (1961).

(15) R. F. Brown, and G. W. McMahon, Can. J. Phys. 40, 672 (1962).

(16) R. F. Brown and G. W McMahon, J. Acoust. Soc. Am. 38, 570 (1965).

The slope $\frac{1}{V}\frac{dV}{dP}$ in the transition region is 2.1 x 10^{-2} m^2/C for the "square" loop composition of Fig. 16 and 3.6 x 10^{-3} m^2/C for the "slanted" loop material of Fig. 15. The six to one ratio is just about equal to the ratio of transition values of $\Delta V/V$. It is also about equal to the ratio of ferroelectric distortions* for these compositions. A truly surprising feature of the "slanted" loop compositions is their very slight distortion from the cubic reference phase in combination with values of P_S about the same as for "square" loop compositions with much higher distortion. It appears either that there are large ionic displacements which do not result in unit cell distortion with the "slanted" loop materials, or perhaps more likely, there is a much larger contribution to the polarization by electron cloud distortion rather than ionic displacements.

Figure 17 shows the dependence of E_f, here defined for a "slanted" loop composition as the electric field at which $P = \frac{1}{2} P_S$, on compressive stress. There is no conclusive difference in the data for hydrostatic stress and parallel stress. There is very little change of E_f with lateral stress. These data were obtained from hysteresis loops taken with stress maintained. Changes of E_a with stress (not shown) are virtually identical, so the difference E_f-E_a is for practical purposes independent of stress.** From the slopes of these curves and the Equations (1), (4), and (5) values of $(\Delta V/V)_t$, $(S_3)_t$, and $(S_1)_t$, with the subscript identifying the strains as transition strains, may be calculated using $\Delta D = P_S$. The values are respectively 0.12%, 0.12%, and 0.028%. Comparison with Fig. 18 for the same nominal composition is fairly difficult since the transition is not sharp, and there are piezoelectric strains in the forced ferroelectric state. The piezoelectric effect is, however, fairly weak. It should nevertheless be noted that the piezoelectric constant d_{31} is very much less in magnitude than d_{33} in the forced ferroelectric state, and as a result the hydrostatic effect $d_h = d_{33} + 2d_{31}$ is considerably stronger than

---

*The ferroelectric distortions are rhombohedral, with the difference in axial lengths of longest and shortest diagonal of the cubic reference cell proportional to the deviation of the rhombohedral angle from 90°.

**There is actually a slight decrease of E_f-E_a with increasing stress.

in ordinary piezoelectric ceramics with perovskite structure. These effects are fairly clear from the slopes of the saturated portions of the curves in Fig. 13. The apparent transition strains in Fig. 13 may be chosen at the electric field at which the polarization saturates, about 30 kv/cm. Neglecting the first one-half cycle they are 0.115% ($\Delta V/V$), 0.10% (S_3), and 0.008% (S_1). Agreement with calculated values is fairly good, especially for $(\Delta V/V)_t$. This would normally be expected; one can achieve exactly hydrostatic conditions, but one can only approach experimentally a condition of one-dimensional stress.

It should be pointed out that direct use of a change of specific volume for generation of acoustic power in a fluid medium cannot be extended to low frequencies without quite large configurations because of the general requirement of dimensions not too small compared to a wavelength. Assuming an isotropic strain in a sphere, the acoustic power in watts is given by

$$p_a = \frac{1}{18} \frac{\left(\frac{2\pi R}{\lambda}\right)^2 c^3 \rho \left(\frac{\Delta V}{V}\right)^2}{\left(\frac{\lambda}{2\pi R}\right)^2 + 1} (4\pi R^2), \quad \text{where} \qquad (12)$$

R = radius, meters
c = velocity of sound (1500 m/sec in water)
ρ = density of water = 10^3 kg/m^3, and
λ = wavelength in meters = c/f .

The antiferroelectric transducer does not generate an isotropic strain even though all strain components are in the same sense (Fig. 13). Nevertheless Equation (12) may be applied to estimate acoustic power available from an antiferroelectric transducer. Table I shows the acoustic power density ($p_a/4\pi R^2$, power per unit area) in water for spheres with several values of R/λ and a volume strain of 0.1%. Cavitation is neglected. Actual values of the radius for the listed values of R/λ are shown for frequencies of 100 and 1000 cps. Corresponding values of total output power are given for all reasonable sphere sizes.

The table also lists values for internally dissipated power. With the slanted "loop" composition of Fig. 12, E_f-E_a is about as low as has yet been achieved, although materials with considerately lower values of E_f are available.

TABLE I

Acoustic power delivered and internally dissipated power for a spherical antiferroelectric radiator with strain assumed isotropic and with $E_f - E_a = 2$ kv/cm, $\Delta P = 15\ \mu C/cm^2$ and $\Delta V/V = 0.1\%$. Cavitation neglected.

R/λ	Output Power/ Unit Area	Radius, cm		Total Output Power, kW		Internally Dissipated* Power, kW		Efficiency %
	Watts/cm^2	100 cps	1000 cps	100 cps	1000 cps	100 cps	1000 cps	
0.02	14×10^{-3}	30	3	0.14	1.4×10^{-3}	51	0.51	0.3
0.05	0.17	75	7.5	11.7	0.12	800	8.0	1.5
0.1	2	150	15	560	5.6	6300	63	8.2
0.2	18.2	--	30	--	206	--	510	29
0.3	52	--	45	--	1320	--	1770	43
0.4	102	--	60	--	3500	--	4200	46

*With 15% of total enclosed volume driven.

In this case $E_f - E_a \sim 2$ kv/cm and $\Delta D \sim 15\ \mu C/cm^2$ for a volume strain of $\sim 0.1\%$ about a bias of ~ 20 kv/cm. The heat power is thus 3 watts/cm^3 at 100 cps or 30 watts/cm^3 at 1000 cps. The total internally dissipated power values listed in Table I were calculated assuming that only 15% of the total enclosed volume is driven. It is immediately evident that the antiferroelectric transducer will require a low duty cycle or forced cooling or both. With a 1% duty cycle and noting that the heat capacity is about 3 $J/cm^3 °C$, the average temperature rise would be about one degree centigrate in 100 seconds at 100 cps or in 10 seconds at 1000 cps, assuming no heat loss. It should be pointed out that optimum compositions from this standpoint (low $E_f - E_a$) have yet to be developed, and there are indications that considerable improvement can be obtained. It is fortuitous that with temperature rise $E_f - E_a$ decreases, with a corresponding decrease in heat power. This can be seen in an extreme example in Fig. 18, where hysteresis loops for a "square" loop composition are shown at several temperatures. With respect to temperature rise, therefore, the antiferroelectric transducer tends to be self-limiting. Narrowing of the loop with the "slanted" loop material is less dramatic but nevertheless definite.

In actual practice one would probably use a stack of rings electrically connected in parallel and with major strain component (Fig. 13) axial. The stack of rings should, of course, be capped to increase fluid displacement. Lateral relief is not required due to the nature of the transition strain. If a horn is provided in order to increase further the fluid displacement, lateral relief would, however, be required.

CONCLUSIONS

The use of an electric field-forced antiferroelectric to ferroelectric transition for electromechanical energy conversion is fairly well understood. Its major advantage is very wideband (nonresonant) operation, and its major disadvantage is high internally dissipated power. It is possible that antiferroelectric transducers may find use in low frequency sonar systems with low duty cycle or as wideband delay line transducers where high strain amplitude is important.

ACKNOWLEDGMENTS

The financial support of Sandia Corporation and Office of Naval Research is gratefully acknowledged. The author wishes to thank B. Jaffe, who developed the ceramic compositions described in this report, and H. H. A. Krueger, who made many of the measurements.

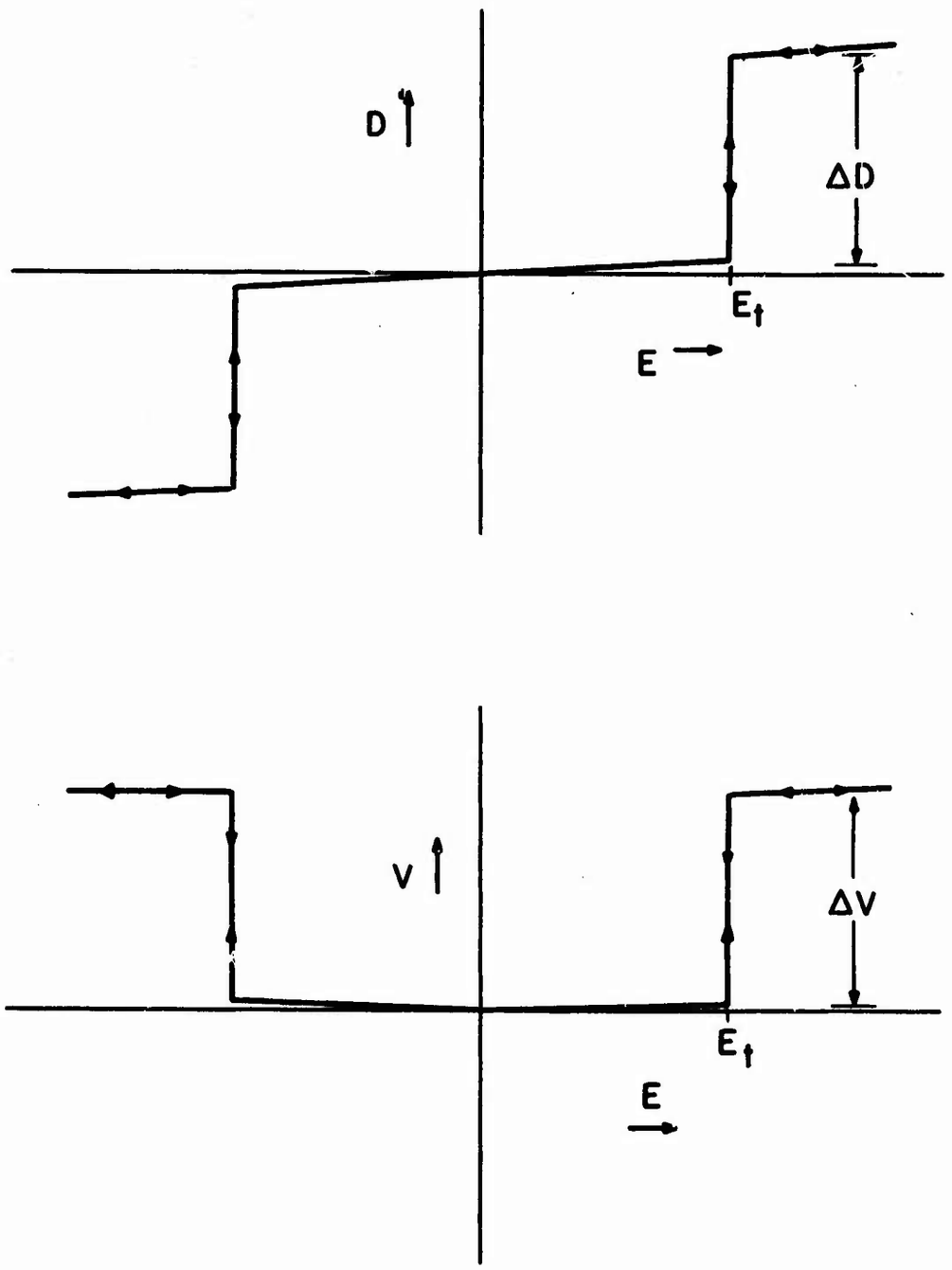

FIG. 1. IDEALIZED ANTIFERROELECTRIC-FERROELCTRIC ELECTRIC FIELD-FORCED TRANSITION

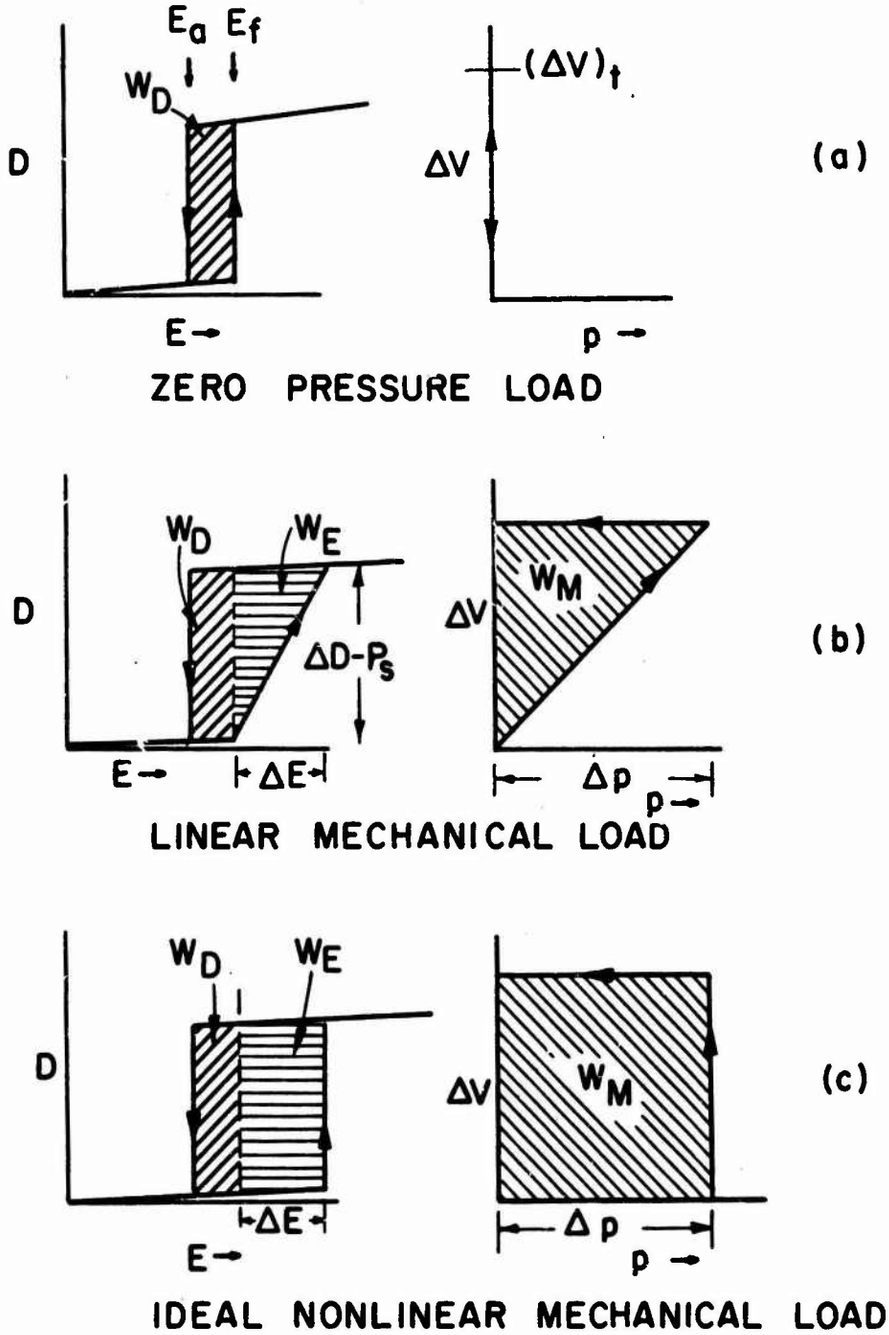

FIG. 2. ANTIFERROELECTRIC TRANSDUCER OPERATION-SCHEMATIC LOAD CYCLE IN (b) AND (c) ASSUMES STORED MECHANICAL ENERGY DISSIPATED.

W_D = ELECTRIC ENERGY DISSIPATED IN TRANSITION CYCLE (HYSTERESIS).

W_E = ADDITIONAL ELECTRIC ENERGY DISSIPATED DUE TO MECHANICAL LOAD.

$W_M = W_E$ = MECHANICAL ENERGY DISSIPATED IN MECHANICAL LOAD FOR THE CYCLE.

ERD 7110

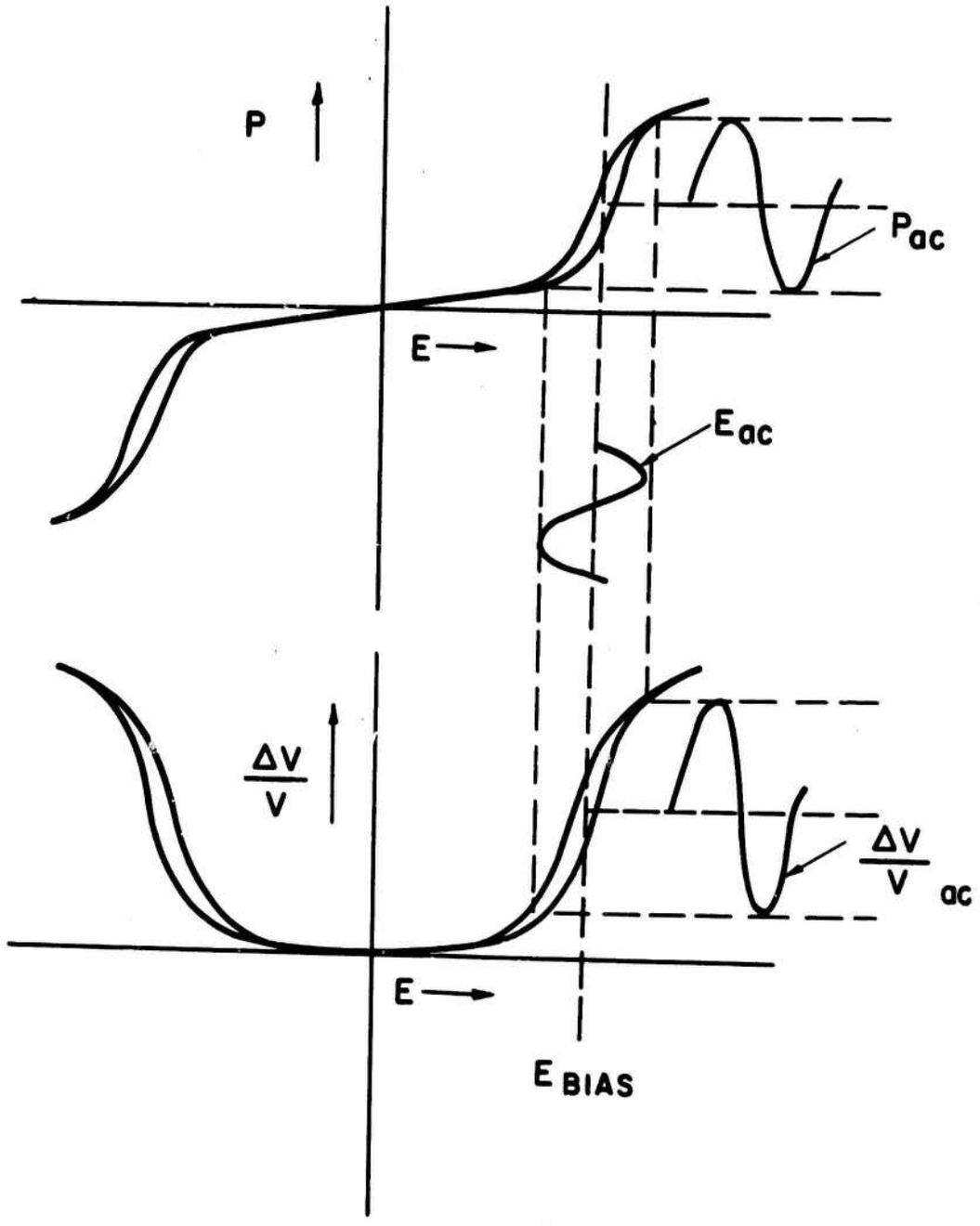

FIG. 3. SCHEMATIC OPERATION OF ANTIFERROELECTRIC TRANSDUCER

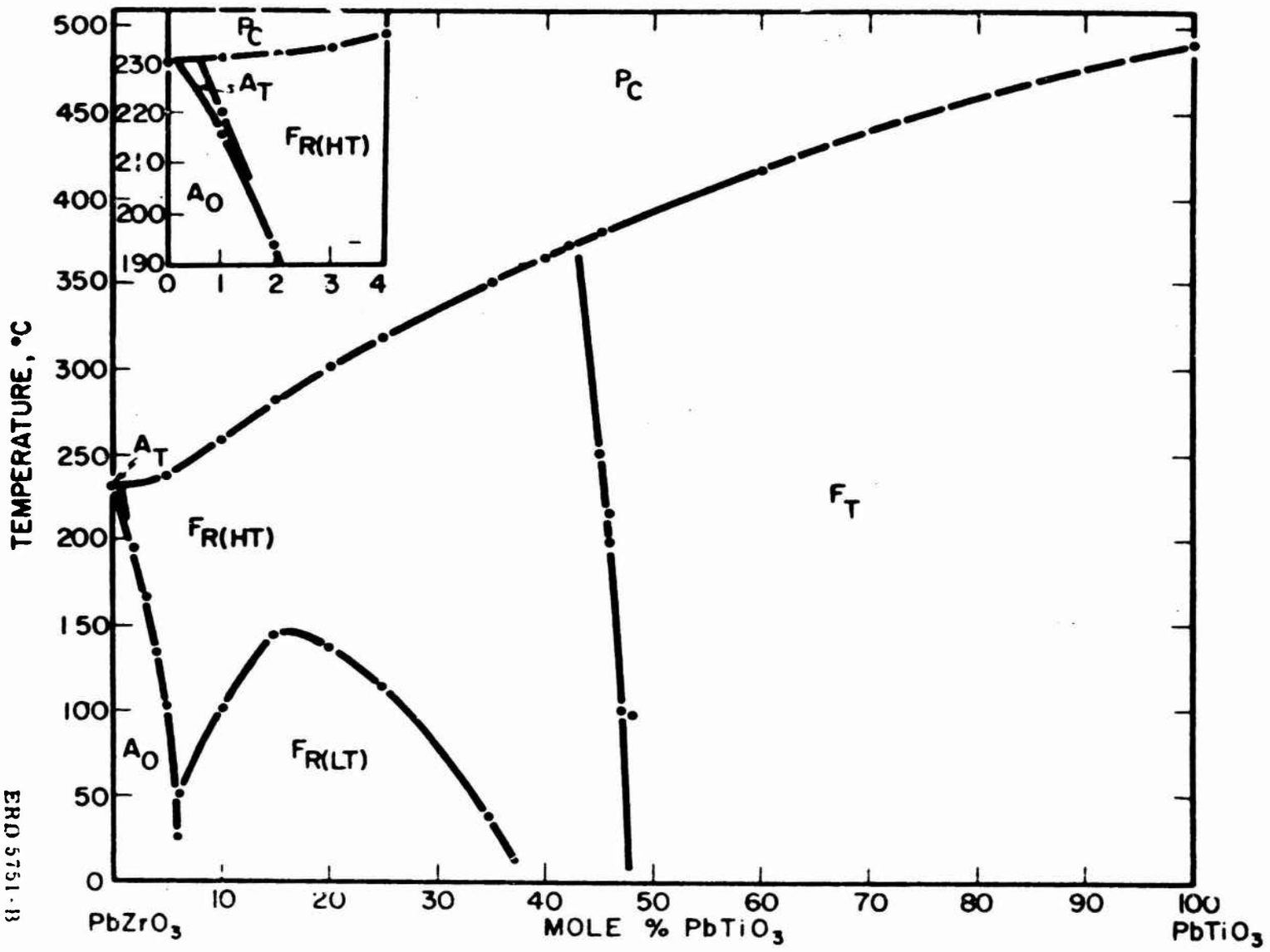

FIG. 4. $PbZrO_3$-$PbTiO_3$ PHASE DIAGRAM

FIGURE 5.

PHASE DIAGRAM

$Pb_{.99}\ Nb_{.02}(Zr,Sn,Ti)_{.98}O_3$

25° C

(POLED AT 25° C IF POSSIBLE)

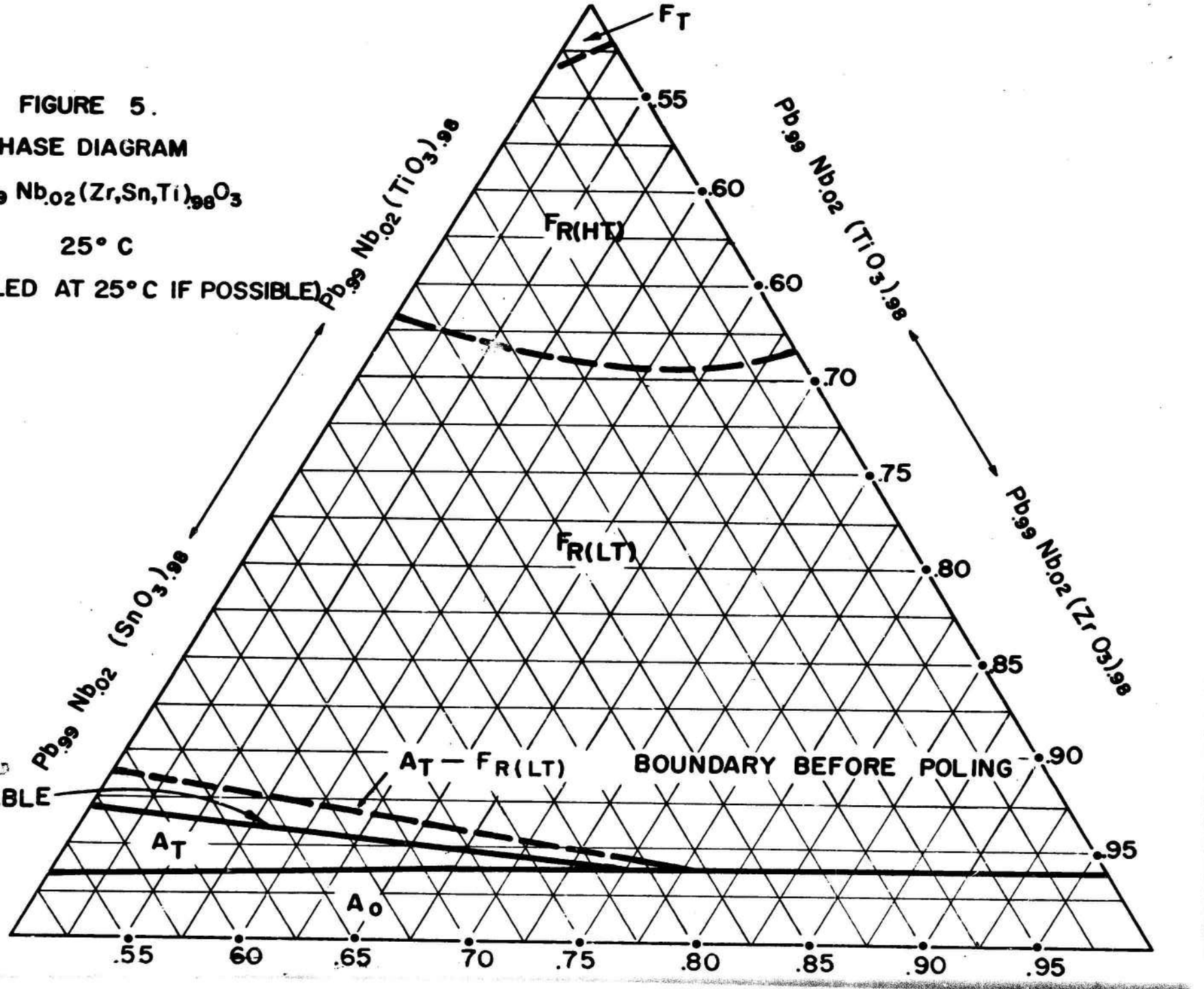

ERD 5650

FIGURE 6
PHASE DIAGRAM

$Pb_{.97}\ La_{.02}\ (Zr, Sn, Ti)\ O_3$

25°C

SPECIMENS NOT POLED

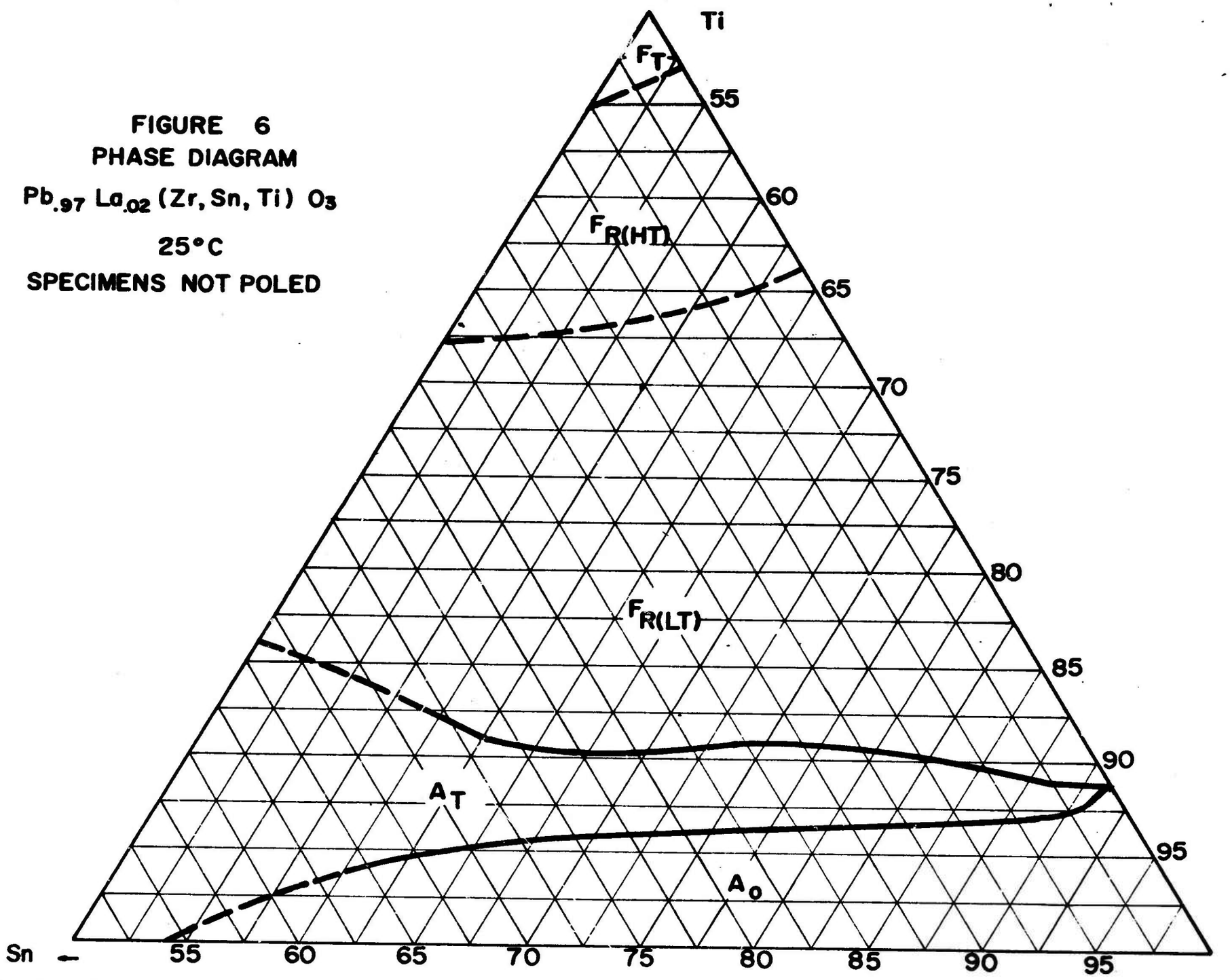

ERD 5651

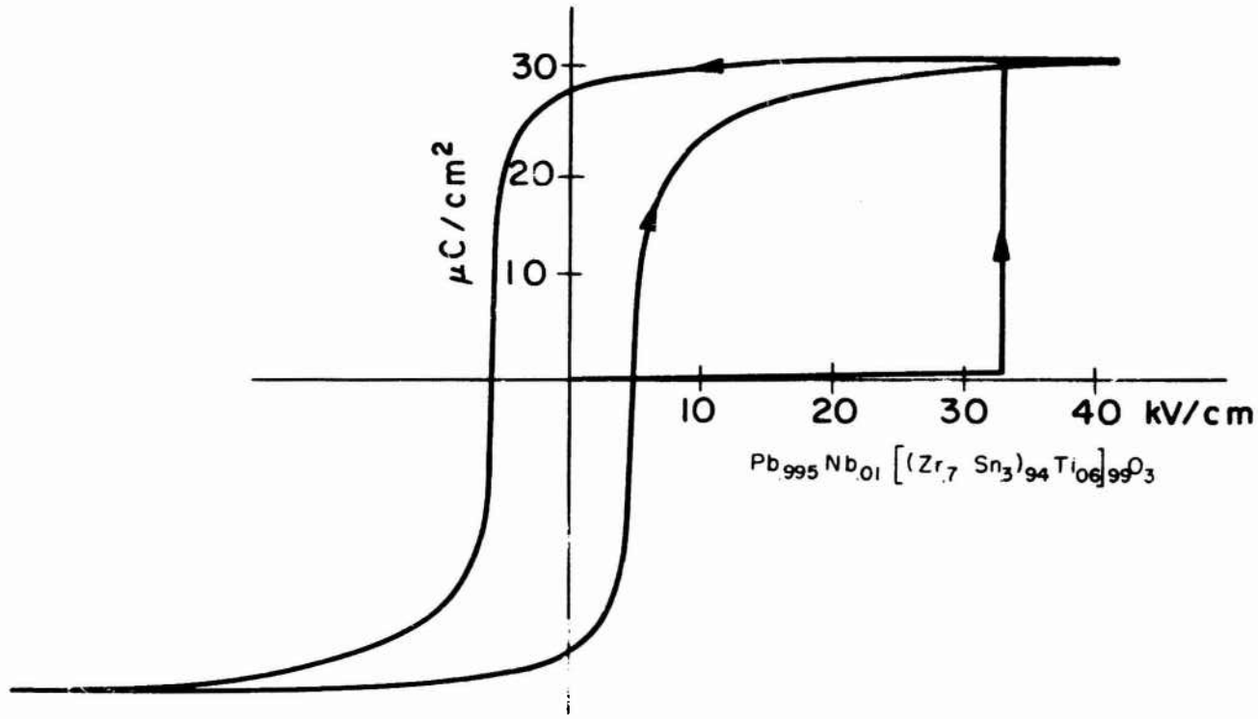

FIG. 7. HYSTERSIS LOOP ILLUSTRATING METASTABLE FERROELECTRIC STATE

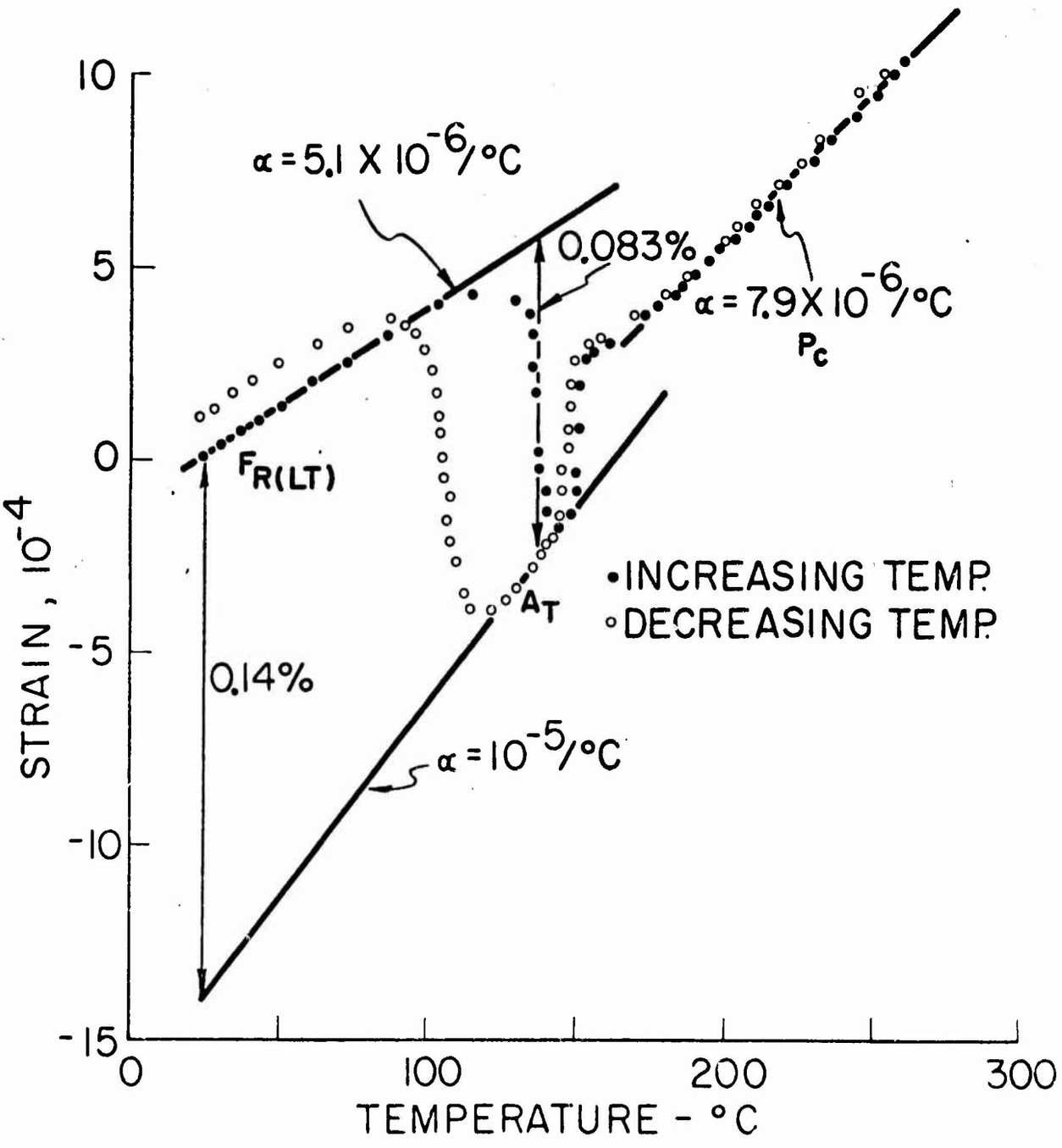

FIG. 8. THERMAL EXPANSION FOR $Pb_{.99}Nb_{.02}(Zr_{.68}Ti_{.07}Sn_{.25})_{.98}O_3$ VIRGIN ELEMENT

ERD 5627

FIGURE 9

THERMAL EXPANSION OF $Pb_{.97}La_{.02}(Zr_{.935}Ti_{.04}Sn_{.025})O_3$

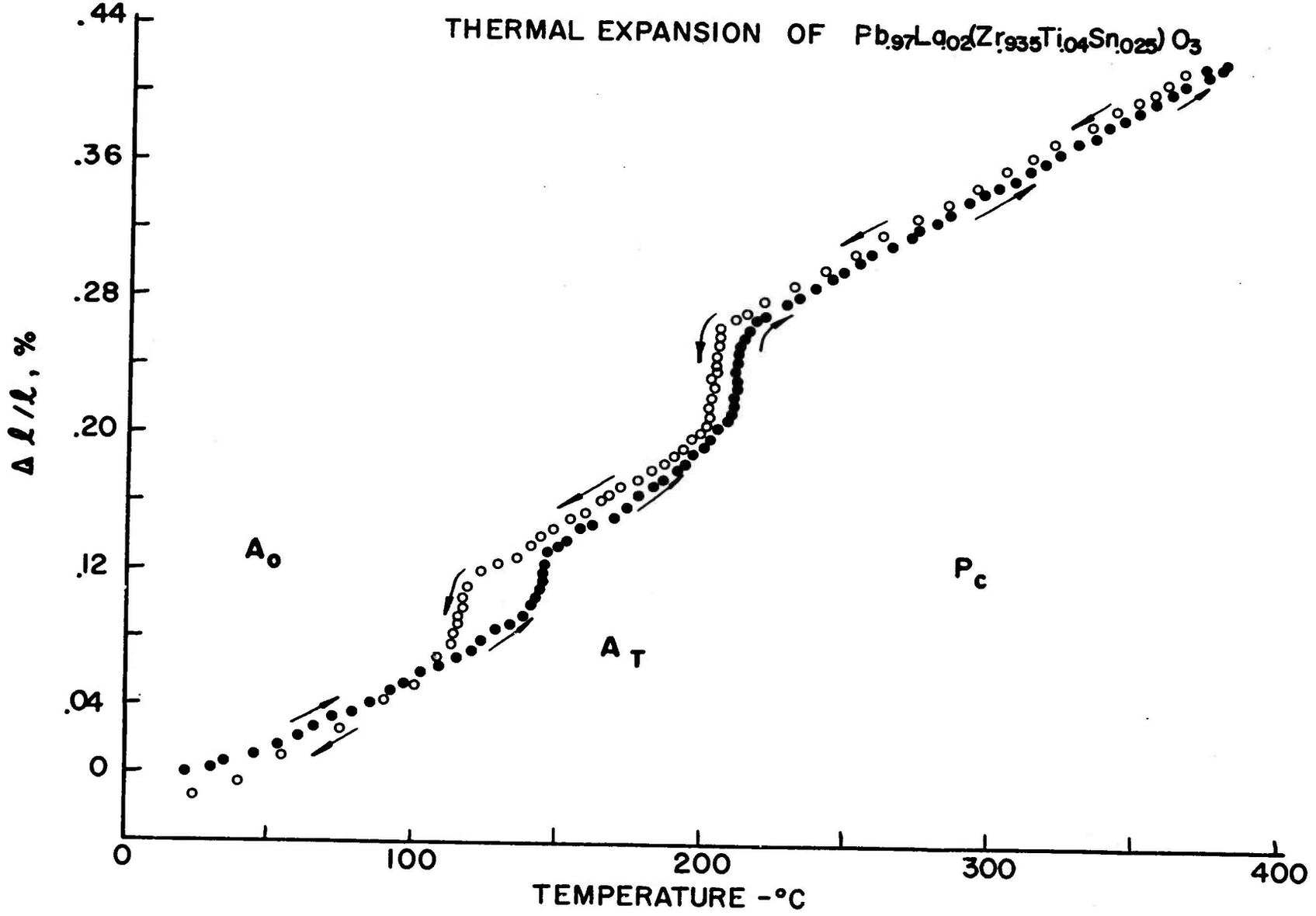

ERD 5403

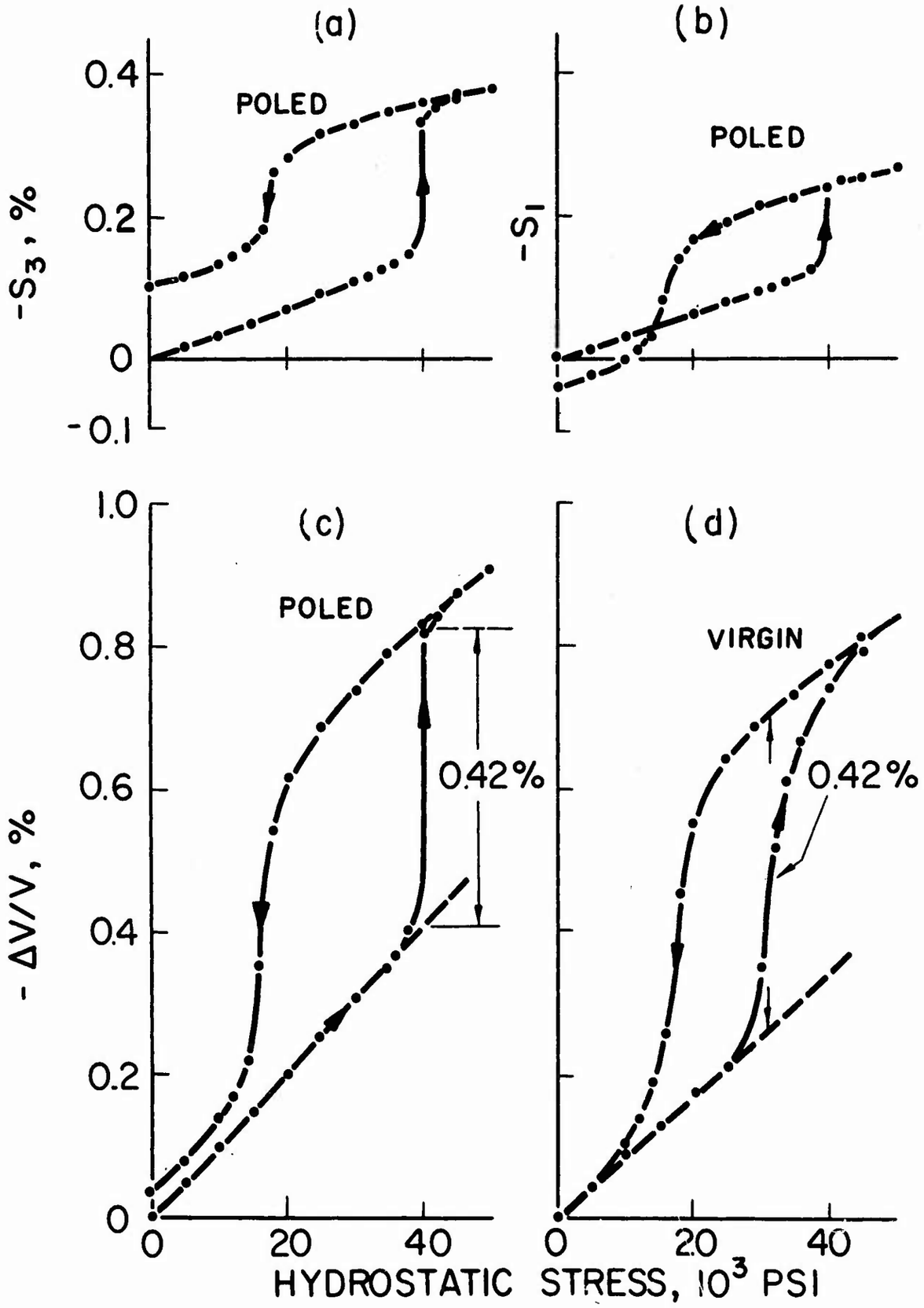

FIG. 10. DIMENSIONAL CHANGES VS. HYDROSTATIC STRESS FOR $Pb_{.99}Nb_{.02}(Zr_{.68}Ti_{.07}Sn_{.25})_{.98}O_3$. LOW AND HIGH PRESSURE PHASES $F_{R(LT)}$ AND A_T

ERD 5628

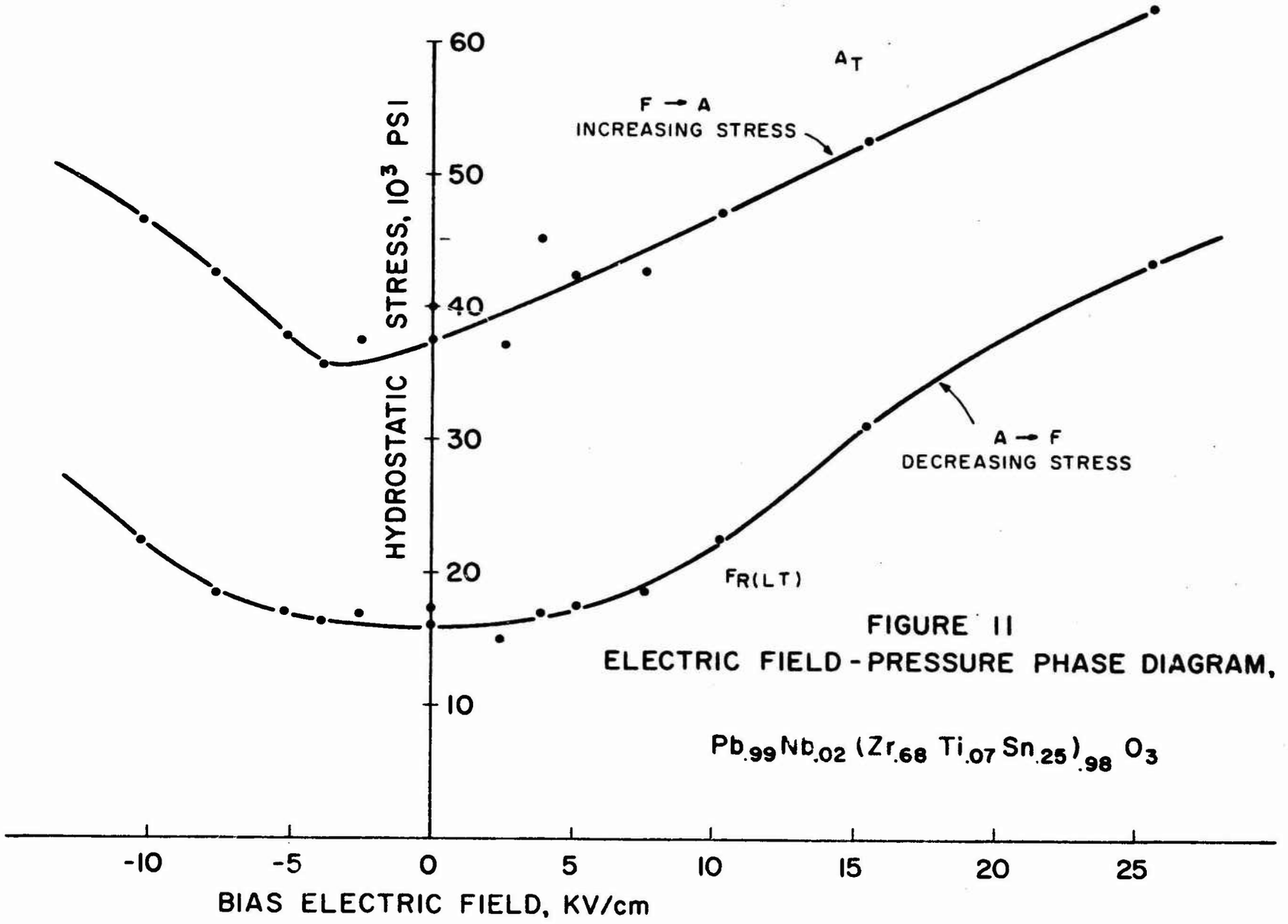

FIGURE 11
ELECTRIC FIELD - PRESSURE PHASE DIAGRAM,

$Pb_{.99}Nb_{.02}(Zr_{.68}Ti_{.07}Sn_{.25})_{.98}O_3$

ERD 5362

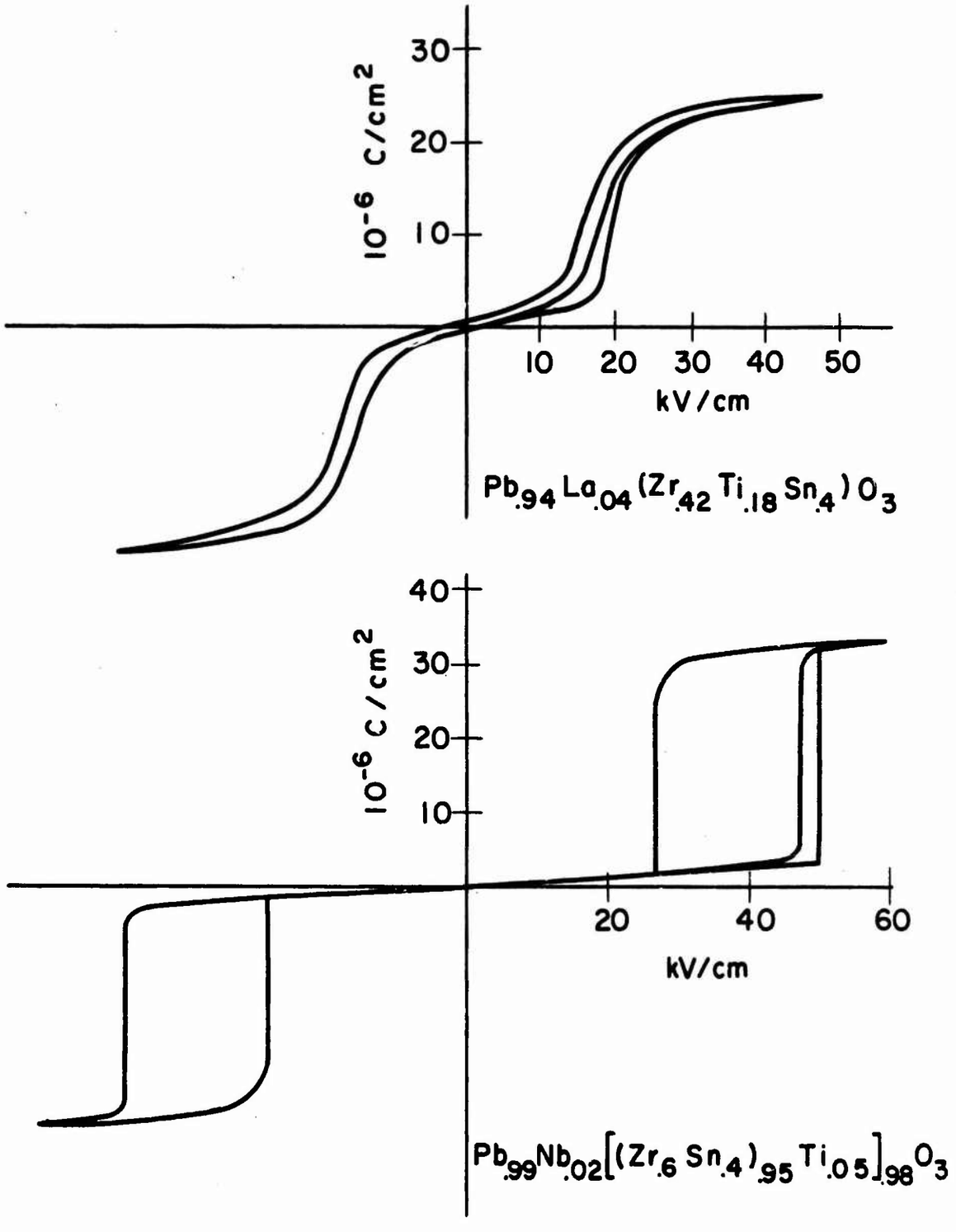

FIG. 12. HYSTERESIS LOOPS

25°C

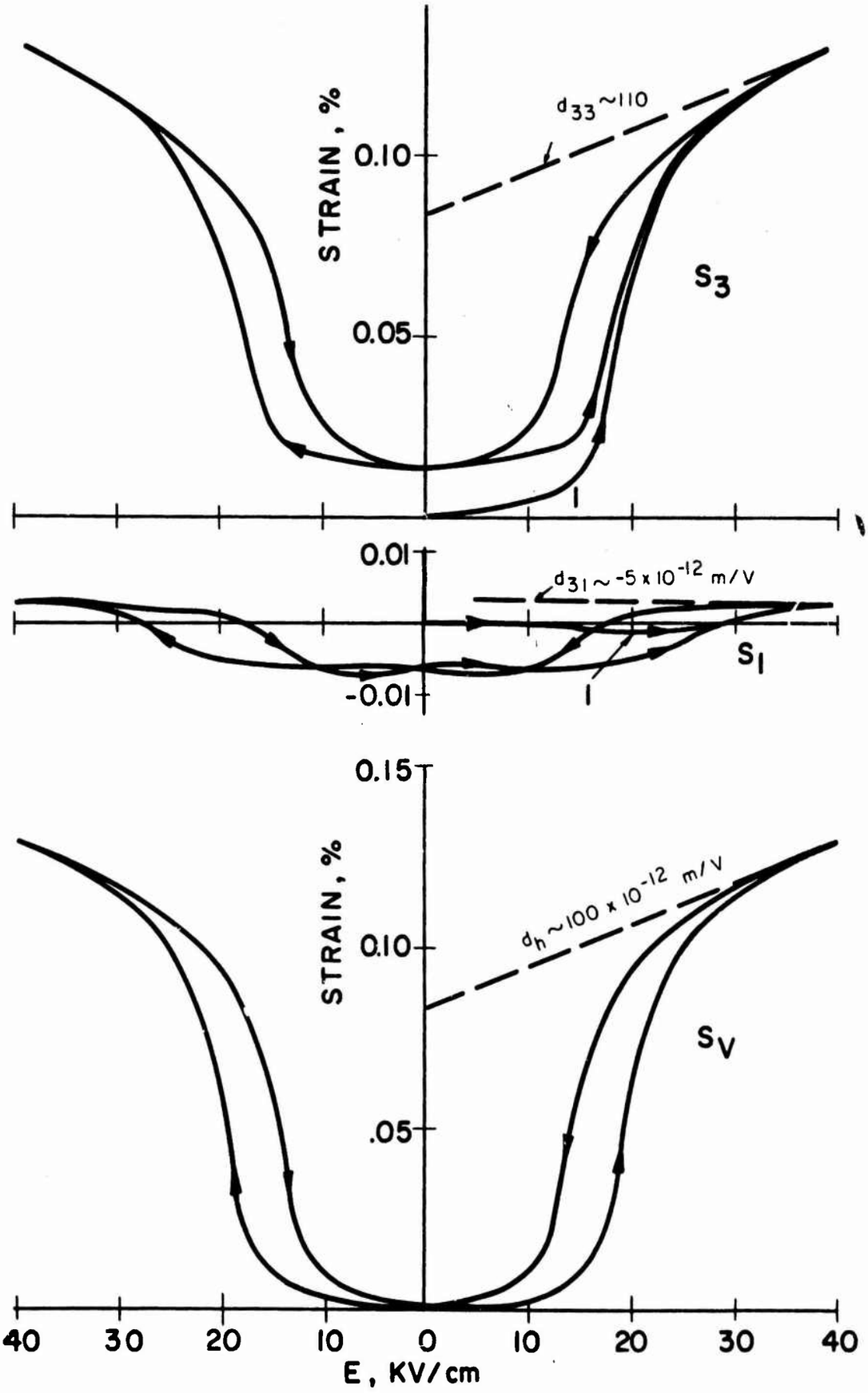

FIG. 13. STRAIN vs. ELECTRIC FIELD THROUGH FORCED TRANSITION CYCLE FOR $Pb_{.94}La_{.04}(Zr_{.42}Ti_{.18}Sn_{.4})O_3$

ERD 7111

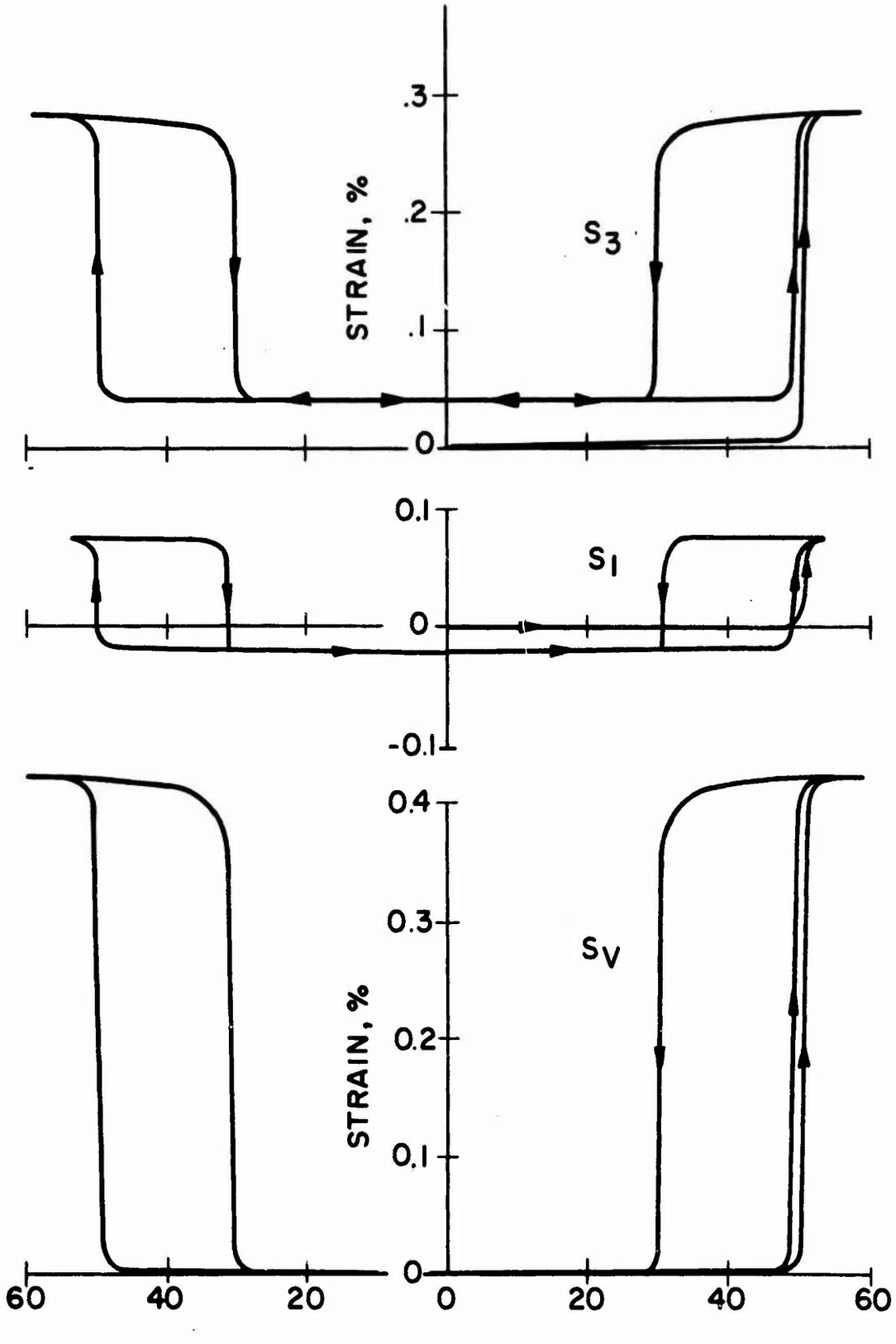

FIG. 14. STRAIN vs. ELECTRIC FIELD THROUGH FORCED TRANSITION CYCLE FOR $Pb_{.99}Nb_{.02}[(Zr_{.6}Sn_{.4})_{.95}Ti_{.05}]_{.98}O_3$

ERD 7112

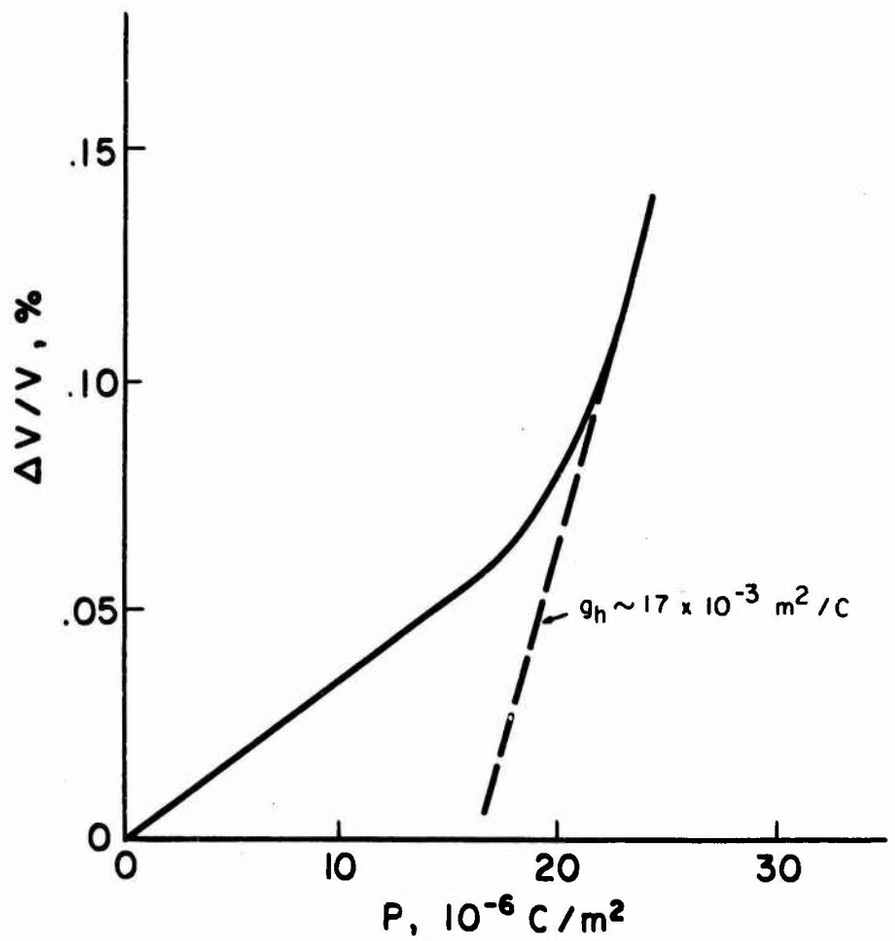

FIG. 15. VOLUME STRAIN vs. POLARIZATION
$Pb_{.94}\ La_{.04}\ (Zr_{.42}\ Ti_{.18}\ Sn_{.4})\ O_3$

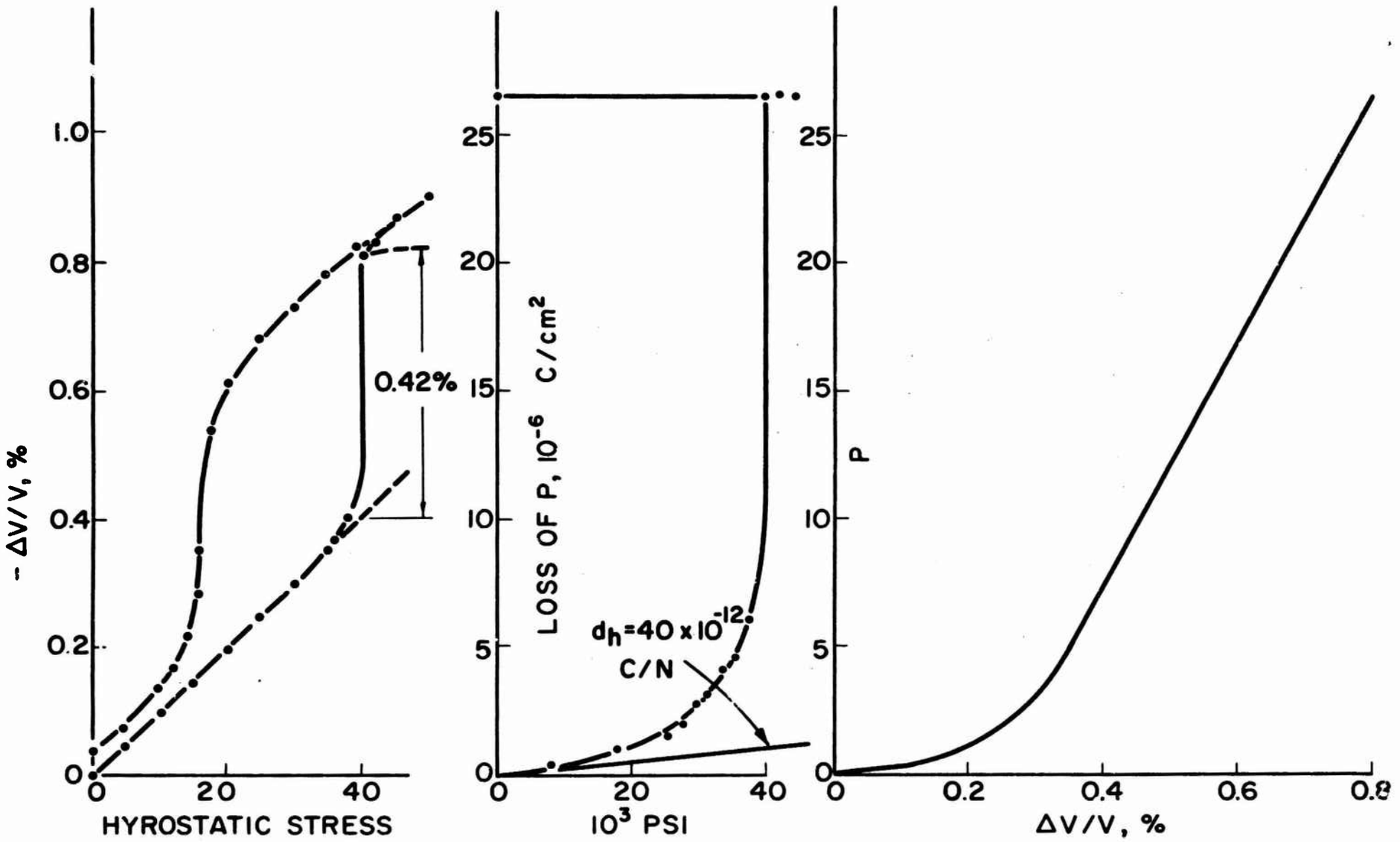

FIG. 16. ΔV/V AND LOSS OF POLARIATION vs. HYDROSTATIC PRESSURE
$Pb_{.99}Nb_{.02}(Zr_{.68}Ti_{.07}Sn_{.25})_{.98}O_3$

ERD 5965

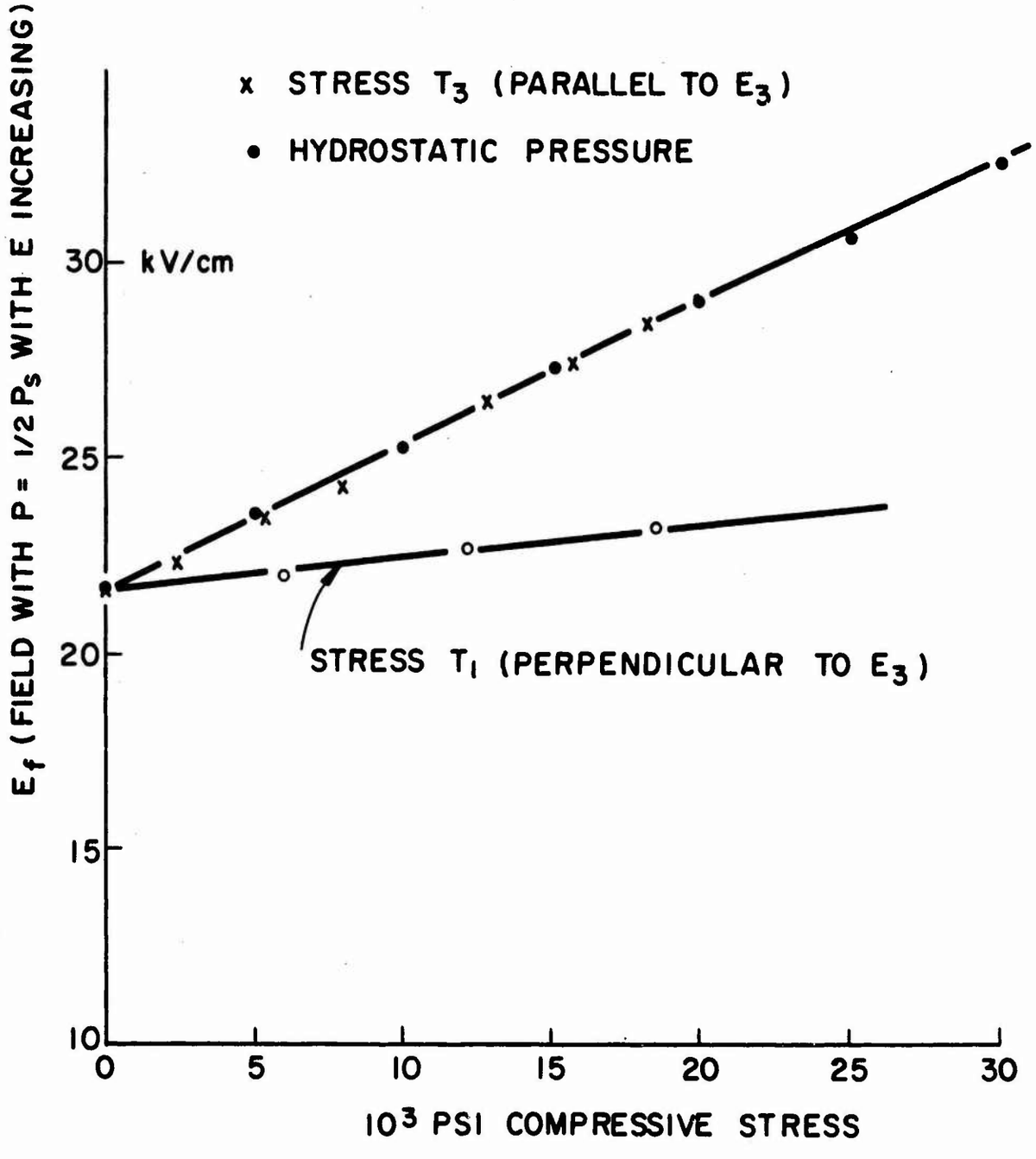

FIG.17. VARIATION OF E_f WITH STRESS FOR $Pb_{.94}La_{.04}(Zr_{.42}Ti_{.18}Sn_{.4})O_3$

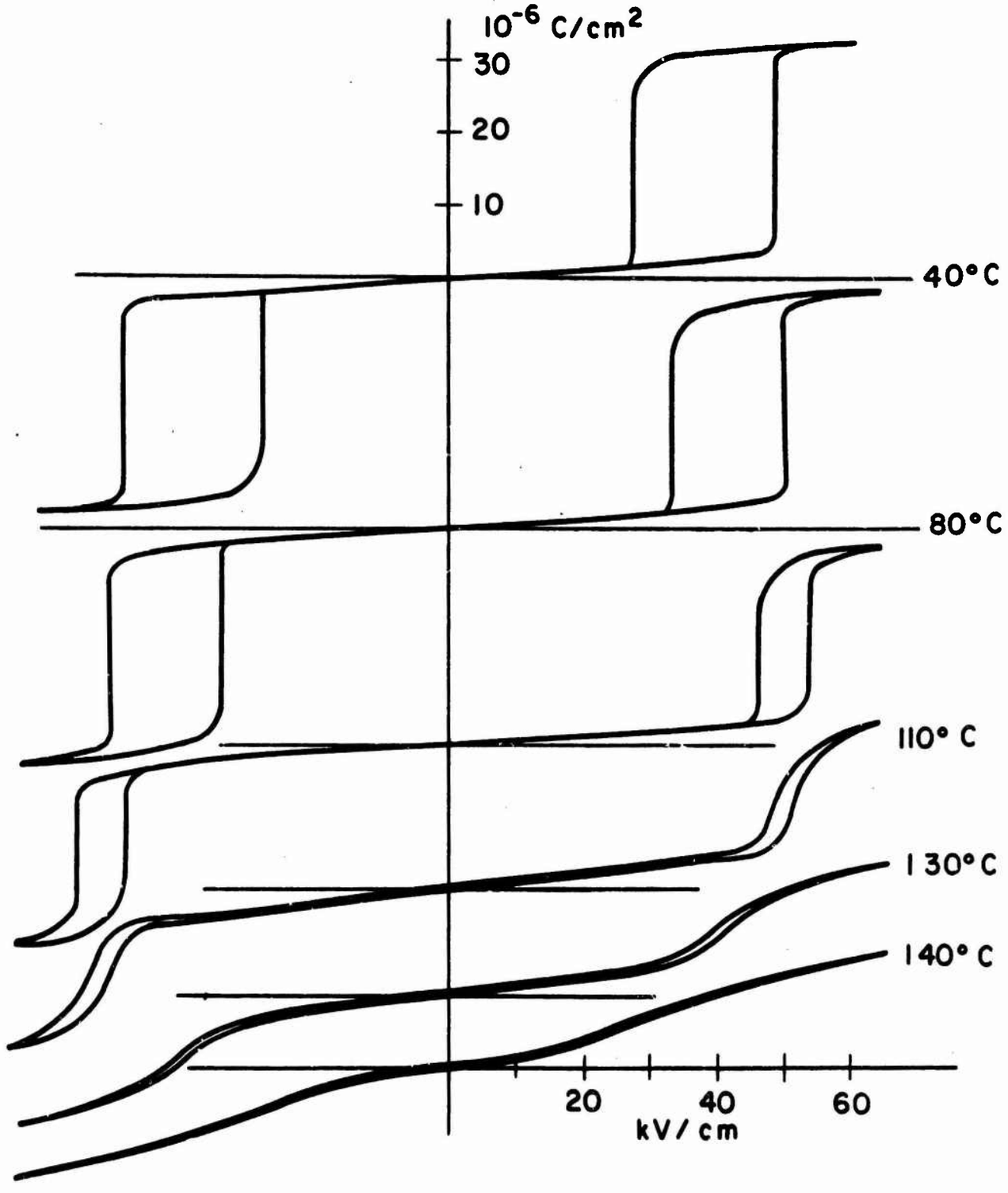

FIG. 18. PROGRESSIVE CHANGE OF HYSTERESIS LOOPS WITH TEMPERATURE ; $Pb_{.99}\,Nb_{.02}\left[(Zr_{.6}\,Sn_{.4})_{.95}\,Ti_{.05}\right]_{.98}O_3$

Unclassified
Security Classification

DOCUMENT CONTROL DATA - R&D

(Security classification of title, body of abstract and indexing annotation must be entered when the overall report is classified)

1. ORIGINATING ACTIVITY (Corporate author)	2a. REPORT SECURITY CLASSIFICATION
Clevite Corporation, Electronic Research Div. 540 E. 105th Street Cleveland, Ohio 44108	Unclassified
	2b. GROUP ---

3. REPORT TITLE

Transducers Using Forced Transitions Between Ferroelectric and Antiferroelectric States

4. DESCRIPTIVE NOTES (Type of report and inclusive dates)

Research report to 1965 Ultrasonics Symposium, IEEE.

5. AUTHOR(S) (Last name, first name, initial)

Berlincourt, Don A.

6. REPORT DATE	7a. TOTAL NO. OF PAGES	7b. NO. OF REFS
December 20, 1965	43	16

8a. CONTRACT OR GRANT NO.	9a. ORIGINATOR'S REPORT NUMBER(S)
Nonr 3958(00) Sandia Corp. (AEC) 53-2206	Engineering Memorandum 65-23
b. PROJECT NO.	
c.	9b. OTHER REPORT NO(S) (Any other numbers that may be assigned this report)
d.	---

10. AVAILABILITY/LIMITATION NOTICES

Qualified requesters may obtain copies of this report from DDC

11. SUPPLEMENTARY NOTES	12. SPONSORING MILITARY ACTIVITY
	Office of Naval Research

13. ABSTRACT

The use of resonant piezoelectric composite structures for acoustic radiation into fluid media is well established. At low frequencies, desirable for long distance acoustic transmission, resonant structures are extremely large and expensive. Frequency lowering can be accomplished by a variety of means involving use of bending structures or mass-loading, but the resulting transducers are vulnerable to pressure effects due to deep submersion. A possible alternative to present transducer structures is the use of the electric field-forced transition from antiferroelectric to ferroelectric. A number of Pb(Zr, Sn, Ti)O_3 compositions have been developed which experience these transitions at relatively low electric field (~ 7-15 kV/cm) and typically generate volume strains near 0.1%. There is therefore not necessarily a requirement for acoustic shielding, and since the developed strain is independent of frequency, resonant structures are not needed. Construction is therefore simplified and the size and weight of low frequency transducers may be reduced. Operating characteristics of the antiferroelectric transducer are discussed in detail, but no large low frequency transducer arrays have yet been built.

DD FORM 1 JAN 64 1473

Unclassified
Security Classification

Unclassified

Security Classification

14 KEY WORDS	LINK A		LINK B		LINK C	
	ROLE	WT	ROLE	WT	ROLE	WT
Transducers Forced transitions Ferroelectric Antiferroelectric						

INSTRUCTIONS

1. ORIGINATING ACTIVITY: Enter the name and address of the contractor, subcontractor, grantee, Department of Defense activity or other organization *(corporate author)* issuing the report.

2a. REPORT SECURITY CLASSIFICATION: Enter the overall security classification of the report. Indicate whether "Restricted Data" is included. Marking is to be in accordance with appropriate security regulations.

2b. GROUP: Automatic downgrading is specified in DoD Directive 5200.10 and Armed Forces Industrial Manual. Enter the group number. Also, when applicable, show that optional markings have been used for Group 3 and Group 4 as authorized.

3. REPORT TITLE: Enter the complete report title in all capital letters. Titles in all cases should be unclassified. If a meaningful title cannot be selected without classification, show title classification in all capitals in parenthesis immediately following the title.

4. DESCRIPTIVE NOTES: If appropriate, enter the type of report, e.g., interim, progress, summary, annual, or final. Give the inclusive dates when a specific reporting period is covered.

5. AUTHOR(S): Enter the name(s) of author(s) as shown on or in the report. Enter last name, first name, middle initial. If military, show rank and branch of service. The name of the principal author is an absolute minimum requirement.

6. REPORT DATE: Enter the date of the report as day, month, year, or month, year. If more than one date appears on the report, use date of publication.

7a. TOTAL NUMBER OF PAGES: The total page count should follow normal pagination procedures, i.e., enter the number of pages containing information.

7b. NUMBER OF REFERENCES: Enter the total number of references cited in the report.

8a. CONTRACT OR GRANT NUMBER: If appropriate, enter the applicable number of the contract or grant under which the report was written.

8b, 8c, & 8d. PROJECT NUMBER: Enter the appropriate military department identification, such as project number, subproject number, system numbers, task number, etc.

9a. ORIGINATOR'S REPORT NUMBER(S): Enter the official report number by which the document will be identified and controlled by the originating activity. This number must be unique to this report.

9b. OTHER REPORT NUMBER(S): If the report has been assigned any other report numbers *(either by the originator or by the sponsor)*, also enter this number(s).

10. AVAILABILITY LIMITATION NOTICES: Enter any limitations on further dissemination of the report, other than those imposed by security classification, using standard statements such as:

(1) "Qualified requesters may obtain copies of this report from DDC."

(2) "Foreign announcement and dissemination of this report by DDC is not authorized."

(3) "U. S. Government agencies may obtain copies of this report directly from DDC. Other qualified DDC users shall request through _____."

(4) "U. S. military agencies may obtain copies of this report directly from DDC. Other qualified users shall request through _____."

(5) "All distribution of this report is controlled. Qualified DDC users shall request through _____."

If the report has been furnished to the Office of Technical Services, Department of Commerce, for sale to the public, indicate this fact and enter the price, if known.

11. SUPPLEMENTARY NOTES: Use for additional explanatory notes.

12. SPONSORING MILITARY ACTIVITY: Enter the name of the departmental project office or laboratory sponsoring *(paying for)* the research and development. Include address.

13. ABSTRACT: Enter an abstract giving a brief and factual summary of the document indicative of the report, even though it may also appear elsewhere in the body of the technical report. If additional space is required, a continuation sheet shall be attached.

It is highly desirable that the abstract of classified reports be unclassified. Each paragraph of the abstract shall end with an indication of the military security classification of the information in the paragraph, represented as (TS), (S), (C), or (U).

There is no limitation on the length of the abstract. However, the suggested length is from 150 to 225 words.

14. KEY WORDS: Key words are technically meaningful terms or short phrases that characterize a report and may be used as index entries for cataloging the report. Key words must be selected so that no security classification is required. Identifiers, such as equipment model designation, trade name, military project code name, geographic location, may be used as key words but will be followed by an indication of technical context. The assignment of links, rules, and weights is optional.

Unclassified

Security Classification